

Video Service Delay Control through Rate Adaptation of Wireless IEEE 802.11a

R. Razavi, M. Fleury, and M. Ghanbari

University of Essex, U.K. {rrazav,fleum,ghan}@essex.ac.uk

Keywords: video services, delay and jitter, wireless rate adaptation.

Abstract

Delay and jitter over a packet network are important considerations for video communication, as display deadlines need to be met. Buffering is a partial solution to such problems on mobile devices, while wireless noise and interference adds to the difficulty. This paper shows how SNR-based rate adaptation is an effective antidote. Related work has mainly considered the impact on throughput rather than delay and IEEE 802.11b rather than 802.11a. Rate adaptation in this paper takes advantage of IEEE 802.11a's physical modes to reduce packet delay and jitter.

1 Introduction

For real-time video communication over the Internet, the impact of packet delay and jitter (variation of delay) is an important issue. For video streaming, the presence of network packet jitter will affect the start-up time, which ideally should be imperceptible. Click-on-Web-clip users are especially delay intolerant. Longer start-up delay results in larger playout buffers, which, when mobile devices are involved, impinges on the memory power budget. Unfortunately, adaptive buffers sensitive to changes in network traffic can result in disconcerting playout discontinuities. When video is combined with speech at the receiver then there is an additional synchronization problem. In [19], a table of tolerable levels of media synchronization levels is given. For example, the maximum tolerable skew for lip synchronization is about 80 ms. For conversational services [22] such as videophone and videoconferencing the requirements for delay are more stringent, ideally no more than 100 ms, leading to the adoption of low-delay codecs. A particular problem is faced in tandem networks, when a wireless interconnect is the last hop on an Internet path, as wireless channels are delay prone. Either packets are retransmitted or packet loss leads to unacceptable video quality at the receiver.

The IEEE 802.11a standard [12] is a high bit-rate variant of IEEE 802.11b, "WiFi", which operates in the unlicensed 2.4 GHz range. Therefore, 802.11a is more suitable for higher-bandwidth video applications. To counter adverse channel condition, the 802.11a standard for wireless LANs has a set of physical modes, which are available to be selected according to channel state. However, the standard does not specify how these physical modes may be used. The packet error rate

(PER) combined with channel delay characteristics all affect the received quality [10] and are dependent on correct choice of mode. Choice of an incorrect rate also reduces the throughput of others sharing the channel [1].

In this paper, we examine the impact of rate adaptation on packet delay and jitter, modelling constant bit rate transport of fixed-size packets, with Medium Access Control (MAC) by the Distributed Coordination Function (DCF) Request to Send/Clear to Send (RTS/CTS) mechanism. In IEEE.802.11, the RTS/CTS mechanism increases the reliability of the Basic Access DCF. The contribution of the paper is extended modelling of IEEE 802.11a packet delay and jitter, as it affects video services, and a proposed scheme of SNR-based rate adaptation that takes advantage of IEEE 802.11a's set of physical modes.

2 Related work

Various mechanisms of rate or link adaptation have been proposed including throughput-based control, implemented in the Atheros' NIC driver for its AR500 chipset [10], Frame-Error-Rate (FER)-based [3], and retry-based [13]. The latter two mechanisms improve the rate of adaptation by directly sampling the channel, while avoiding oscillation between modes. However, there is the possibility of extra contention for the medium and pessimistic mode choices due to error bursts. Signal-to-Noise Ratio (SNR)-based rate adaptation [10][11] has the advantage that an appropriate mode is directly chosen, without stepping up or down the modes. Given SNR vs. goodput (non-errored throughput) curves encapsulated in a look-up table, for example available from [17][6], an implementation selects the mode that gives the optimum goodput in a given circumstances (with some variation due to fragmentation [17] and number of stations [6]). In [11], the receiver estimates the channel condition (number of multipath components, symbol error rate, signal strength) from the initial (RTS/CTS) handshake exchange and use of the ACK frame is another possibility [15].

3 Background

3.1 Medium Access Control with RTS/CTS

The DCF RTS/CTS extension to the IEEE 802.11 MAC seeks to minimize delay from collisions and reduce the problem of out of range (hidden) stations. Its features are briefly summarized, with further details available from for

example [5]. Stations contend for access through the DCF to the RF channel using a Carrier Sense Multiple Access mechanism with Collision Avoidance (CSMA/CA). RTS and CTS frames, carrying the length of the expected data packet, are exchanged before data transmission occurs. If the medium is free for a DCF Inter-Frame Spacing (DIFS) a station begins transmitting an RTS frame and similarly, after a Short Inter-Frame Space (SIFS), the CTS is returned from the destination. At each stage of this exchange, a Network Allocation Vector (NAV) is configured by listening stations that detect one or more of the exchanges to the duration of the expected data transmission with acknowledgment. If collisions occur during the negotiation, as no CTS is returned, a transmitting station exponentially backs off in a way that avoids repeated collisions, while fairness between contending transmitters is ensured.

3.2 Physical modes

IEEE 802.11a Orthogonal Frequency Division Multiplexing (OFDM) across 20 MHz channels supports eight physical modes on 52 sub-carriers, according to modulation and coding rate. Table 1 analyses the rates according to the mandatory channel coding schemes.

M o d e	Bit Rate (Mbps)	Mod- ulation	Coding rate	N_{BPSC}	N_{CBPS}	N_{DBPS}
1	6	BPSK	1/2	1	48	24
2	9	BPSK	3/4	1	48	36
3	12	QPSK	1/2	2	96	48
4	18	QPSK	3/4	2	96	72
5	24	16-QAM	1/2	4	192	96
6	36	16-QAM	3/4	4	192	144
7	48	64-QAM	2/3	6	288	192
8	54	64-QAM	3/4	6	288	216

N_{BPSC} = no. of coded bits per sub-carrier, N_{CBPS} = no. of coded bits per OFDM symbol, N_{DBPS} = no. of data bits per OFDM symbol. N.B. 4 sub-carriers are used as pilots.

Table 1: Physical modes of IEEE 802.11a.

Notice that in Europe, IEEE 802.11g is a similar OFDM system but operates at 2.4 GHz, where it is more prone to interference but has a slightly longer range (~35 m to ~30m).

OFDM is relatively immune to inter-symbol interference and multipath effects unless multipath is combined with Doppler frequency shift [14], caused by relative motion. This is because OFDM requires strict frequency synchronization.

4 Methodology

4.1 Channel model

By means of a Gilbert-Elliott (G.-E.) RF channel model [7], two SNR states were simulated in our experiments. Though

these states lead to the selection of adjacent physical modes (in terms of supported bit rates), equally any two modes could have been selected and, hence, the results are completely general. The SNR ranges chosen are consistent with the literature and a chipset implementation.

The mean duration of a G.-E. good state, T_g , was set at 200 ms and for a bad state, T_b , was set to 50 ms, which settings are similar to those in [8]. In

$$T_g = \frac{1}{1 - P_{gg}}, T_b = \frac{1}{1 - P_{bb}}, \quad (1)$$

given that the current state is g, P_{gg} , the transition probability that the next state is also g, was set to 0.9950 and, given the current state is b, P_{bb} , the transition probability that the next state is also b, was 0.9800.

The two transition probabilities are chosen to correspond to two E_b/N_0 's for which modes 5 and 6 of IEEE 802.11a provide optimal goodput. In [17] for two stations, curves for E_b/N_0 vs. goodput (the amount of data successfully received by the application, excluding headers and error coding overhead) suggest that mode 5 (Table 1) is optimal from about 12 dB, to about 16 dB, while mode 6 is optimal from between 16 dB to 18 dB. Interestingly, the Atheros AR500 chipset [20] is reported as operating under similar SNR conditions to [17], at least in the higher physical modes, with mode 5 operating from 11.3 to 14.9 dB and mode 6 between 14.9 and 18.6 dB. In [10], a refinement introduces a higher lower threshold when channel conditions are adjudged to be volatile and overlapping ranges occur, which is probably a necessary adjustment in practice (though not applied in the simulations reported herein).

In [6], with similar decision points between these two modes for two stations, the ten station result is also given, indicating that it is principally the achievable goodput that is affected by an increase in stations rather than a change in the SNR vs. mode levels. One factor in the decline in goodput is clearly increased contention for the shared channel as the number of stations increases.

4.2 Simulation environment

The simulator, which models the MAC layer, was adapted from an earlier design by us [18] to IEEE 802.11a. Notice that the MAC implementation in the well-known ns-2 simulator is reported [21] to contain several bugs. In our simulator, ten runs were averaged for each data point and 20000 packets were transmitted in each run. The default IEEE 802.11 settings for the discrete event simulations are recorded in Table 2.

RTS length	160 bits
CTS length	112 bits
ACK	112 bits
Physical header	48 bits
MAC data header	224 bits
SIFS	10 μ s
DIFS	50 μ s

Table 2: Fixed parameters for the simulations.

In the simulations, not only the access delay but the queuing delay at the transmitter is accounted for. However, to isolate relevant results, the transmitter queue length was set to a size that avoided all packet loss. A FIFO queue discipline was applied. In practice buffer overflows may occur, which would decrease the delays reported herein but would also decrease the quality of service for a multimedia application. The simulations also include the (deterministic) service time to send a data packet, but do not include a further delay, as far as the transmitter is concerned, in receiving a final acknowledgment. This is because, for real-time video services, once the data are received at the destination, processing can commence. The WLAN is assumed to be in infrastructure mode, with all transmissions sent to the base station. Scheduling time at the base station is neglected in the simulations in Section 5.

5 Results

5.1 Without adaptation

This Section reports for mode 6 operation basic results without rate adaptation but according to a given PER. PERs are available in equation form from [17][16] and [9]. By default, packet arrival rate was set at 200 packet/s per station and ten stations were simulated. The settings are summarized in Table 3, though individual simulations vary one or more of these parameters (except packet size). The results in this Section are based on collision rates, as clearly these dynamically impact delay.

Number of stations	10
Packet arrival rate/s	200
Packet arrival distribution	Poisson
Transmission rate	36 Mbps
Packet size	256 B

Table 3: Parameters for simulations

Fig. 1 shows the effect of arrival rate changes on the collision rate. The plots show that the collision rate suddenly increases when the offered load exceeds 1500 packet/s. At this point, almost all stations have some packets to transmit. From then on increasing the arrival rate at each station can only cause the station's buffer to grow, though this is hidden from the channel. Any further increase in the offered load affects the queuing delay of the packets. For the same offered load, a greater PER implies a greater number of packets are retransmitted, in effect resulting in a greater offered load. For this reason, as the Figure shows, the effect of an increase in the PER is simply a vertical shift of the graph.

The PER also affects the RTS/CTS and ACK frames but these are transmitted at a control rate, either 6, 12, or 24 Mbps, to increase the reception range that stations can detect their presence, and their small size increases noise immunity. However, combining a lower control rate with a higher data mode does not necessarily give favourable performance

relative to Basic Access [4] for small numbers of stations (around 5). The simulations do not use the lower rate control modes but for the small packet size (256 B) assumed by us and others, e.g. [6], RTS/CTS performance may not be optimal, as may also be implied from the Bianchi model [2], which was validated at the lower transmission rates of IEEE 802.11b.

Fig. 2 shows the impact of increasing the number of stations upon the collision rate. The collision rate grows considerably as the number of stations is increased. Again, at a certain point the slope of the plots rises steeply as the channel approaches saturation. For a very large number of stations, above 100, the effect of PER is not important but simply results in a higher number of retransmissions. Unlike arrival rate increases, when the number of stations increases there is no plateau beyond which the number of collisions stabilizes.

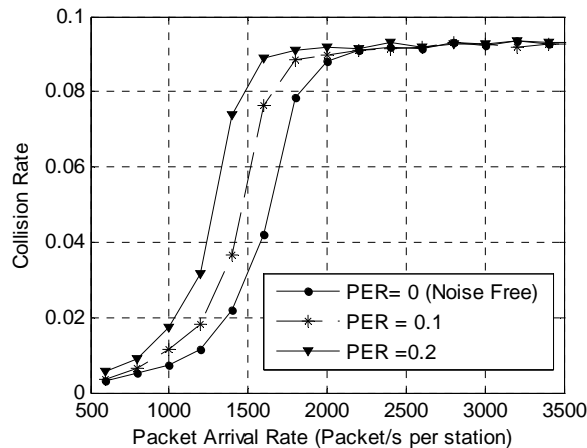


Figure 1: Packet arrival rate vs. collision rate.

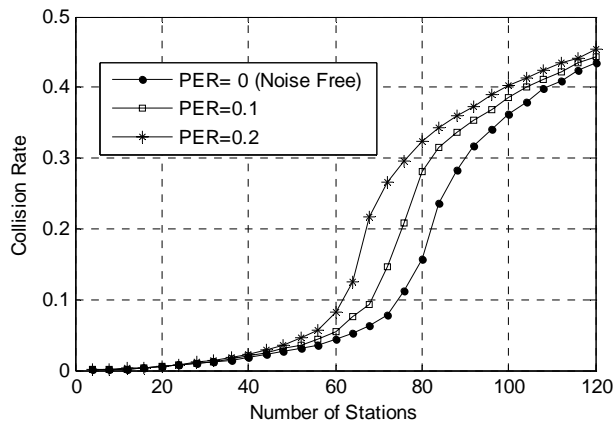


Figure 2: Number of stations vs. collision rate.

5.2 With adaptation

In this Section, rate adaptation is modelled in scenario one by choosing mode 5 at a bit rate of 24 Mbps if the SNR is 14 dB and mode 6 at a rate of 36 Mbps if the channel SNR is 16 dB. The two channel states are represented by the G.-E.

model of Section 4.1. The PER model is the same as for the previous Section. By the G.-E. model, state b has $PER = 0.04$ and state g has $PER = 5 \times 10^{-8}$. By way of comparison, delay for an error-free channel is presented in scenario two, along with delay if no adaptation is applied in scenario three. The default simulation settings are the same as in Tables 1 and 2.

Fig. 3 plots the three scenarios. Delay rises with an increase in the packet arrival rate and more interestingly it can be seen that after a certain level, which corresponds to the maximum available goodput of the channel, the delay starts increasing in an exponential manner (the graph scales are logarithmic). Under noisy conditions, rate adaptation results in the least delay and in that respect the rate adaptive method can handle a larger range of offered load.

The effect of an increasing number of stations upon delay is analyzed in Fig. 4. As is self-evident, a similar discussion applies to an increase in number of stations as it does to packet arrival rate.

In summary, rate adaptation is most effective when the channel is well utilized. The effect is less apparent otherwise and a similar observation applies to the impact on jitter as developed hereafter.

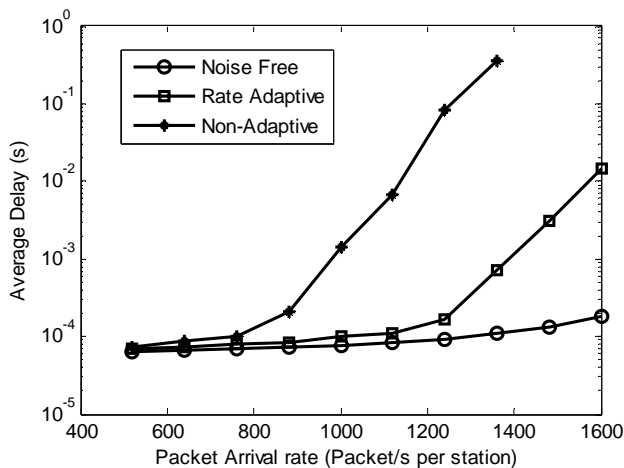


Figure 3: Packet arrival rate vs. delay, with and without rate adaptation (note vertical logarithmic scale).

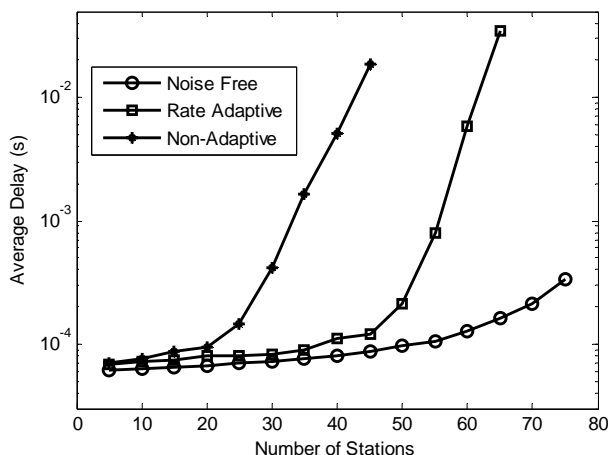


Figure 4: Number of stations vs. delay, with and without rate adaptation (note the logarithmic vertical scale).

In Fig. 5 (a), the variation of the delay over a sequence of 3000 packets of size 256 bytes is noticeable, because of the random occurrence of bad states in the G.-E. channel. During a bad state, packets need to be retransmitted, which leads to an increase in delay both for the retransmitted packets and those waiting in the buffer. When rate adaptation is applied, Fig. 5 (b), the variation is considerably reduced, though, because the lower bit rate may be chosen, the general level of delay is above that of Fig. 5 (a).

The mean ratio of time spent in the bad state to overall time, i.e. $T_b/(T_b+T_g)$, is varied in Fig. 6 to gauge the general effect of rate adaptation, which consistently improves jitter. However, Fig. 6 simulates the lightly loaded channel of Table 2's settings, whereas Fig. 7 models a heavily loaded network. It is apparent that very serious levels of jitter occur if rate adaptation is not implemented. In summary, jitter is highly sensitive to channel load but can be considerably improved by rate adaptation.

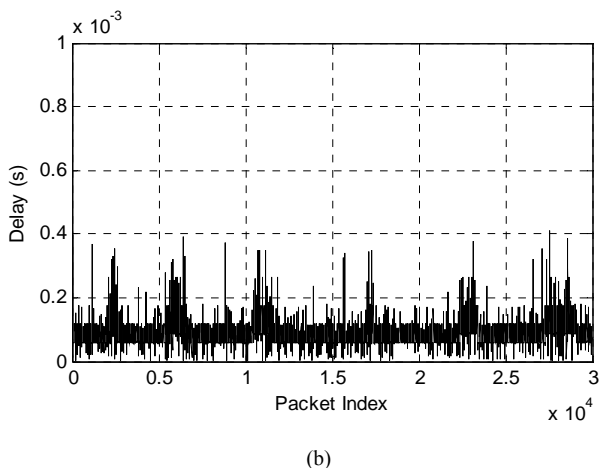
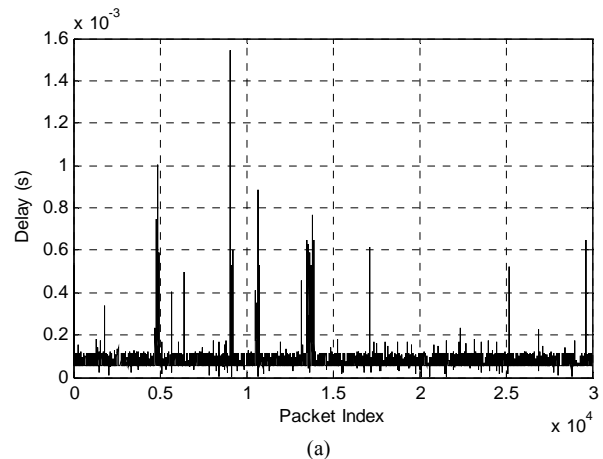


Fig. 5 Variation in packet delay over 3000 packets, (a) without rate adaptation (b) with rate adaptation.

5.3 Discussion

The Cumulative Distribution Functions (CDFs) of delay for a variety of different scenarios discussed previously are

shown in Fig. 8. Distinguishing between rate adaptive and non-rate adaptive plots for equivalent conditions, the most delayed packets at the 90th percentile (last 10%) experience greater delays (and/or jitter) if adaptation is not implemented. While rate adaptation tends to results in greater delays for those packets below the 90th percentile, the delay is at such a level to be of limited effect. The greater range of delays for non-adaptive plots in Fig. 8 also reflects the greater levels of jitter experienced by packets for this form of transmission.

Lastly, it is worth remarking that rate adaptation has an important effect on power consumption, as Fig. 9 illustrates. In the Figure, for a network with Table 2's settings, as $T_b/(T_b+T_g)$ increases, the success transmission rate linearly and significantly declines. In practice, this causes repeated retries which increases power usage and is also a reason to prefer rate adaptation based on an SNR measure of channel state to those using some form of statistical measure. Clearly, a video clip will be unwatchable if the mobile station is unable to operate!

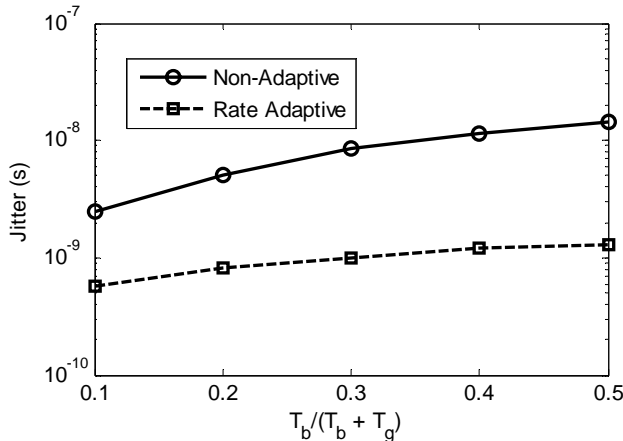


Figure 6: Variation in packet delay for a lightly loaded channel (200 packet/s per station)(note the vertical logarithmic scale).

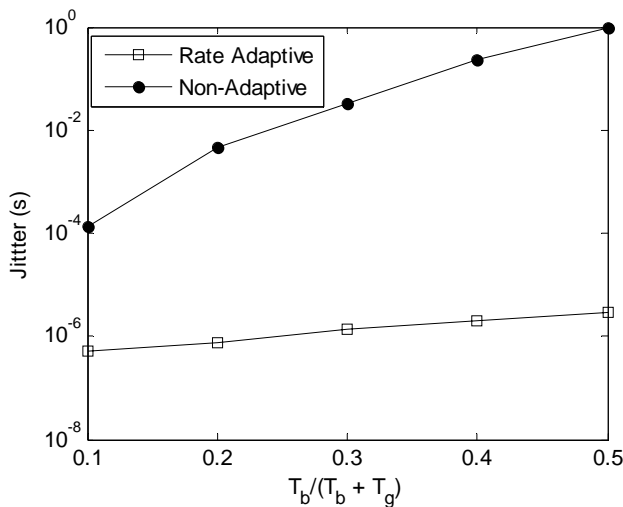


Figure 7: Variation in packet delay for a heavily loaded channel (1000 packet/s per station) (note the vertical logarithmic scale).

6 Conclusions

For real-time video services this study exposes a risk of quality degradation under unfavourable channel state and load conditions, despite the relative high bit rates of the IEEE 802.11a variant. However, rate adaptation, as developed in this paper, is an effective solution to these problems at a small cost in slightly increased average delay at low channel loadings. The paper contributes a rate adaptation method especially tailored to the IEEE 802.11a variant, which is suited to video streaming applications.

When channel load and/or packet error rate rises, considerable delay occurs and there is the possibility of large values of jitter. This effect has been demonstrated for transitions between two adjacent IEEE 802.11a physical modes, whereas swings in channel conditions may be larger in practice, resulting in larger delay/jitter values if an incorrect mode is chosen. Because the effect studied may be stronger in practice and rapid rate adaptation is needed (though not oscillation), this points to an SNR-based rate-control mechanism, as advocated by the paper.

Acknowledgements

This work was supported by the EPSRC, UK under grant no. EP/C538692/1.

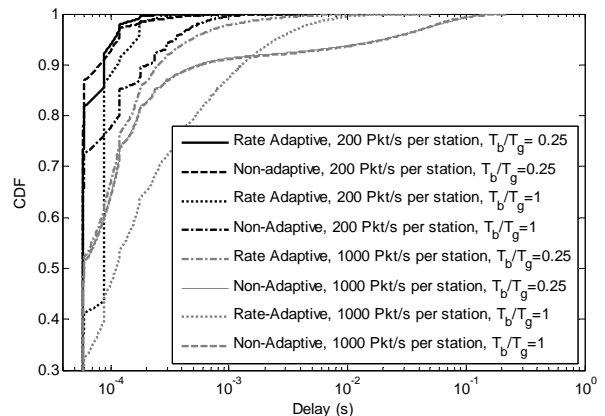


Figure 8: Cumulative Distribution Function (CDF) of delay for various packet arrival rates with and without rate adaptation (note the horizontal logarithmic scale).

References

- [1] K. Balachandran, S. Kadaba, and S. Nanda, "Channel Quality Estimation and Rate Adaptation for Cellular Mobile Radio", *IEEE J. in Selected Areas in Comms.*, vol. 17, no. 7, pp. 1244-1256, (1999).
- [2] G. Bianchi, "Performance Analysis of the IEEE 802.11 Distributed Coordination Function", *IEEE J. on Selected Areas in Comms.*, vol. 18, no. 3, pp. 535-547, (2004).
- [3] B.E. Braswell and J.C. McEachen, "Modeling Data Rate Agility in the IEEE 802.11a WLAN Protocol", *OPNETWORK 2001*, (2001).
- [4] P. Chatzimisios, A. C. Boucouvalas, and V. Vitsas, "Effectiveness of RTS/CTS handshake in IEEE 802.11a

Wireless LANs”, *Electronic Letters*, **vol. 10, no. 14**, pp. 915-916, (2004).

[5] P. Chatzimisios, V. Vitsas and A.C. Boucouvalas, “Throughput and Delay Analysis of IEEE 802.11 Protocol”, *IEEE 5th Int. Workshop on Networked Appliances*, pp. 168-174, (2002).

[6] K.-Y. Doo, J.-Y. Song and D.-H. Cho, “Enhanced Transmission Mode Selection in IEEE 802.11a WLAN System”, *IEEE Int. Vehicular Tech. Conf.*, **vol. 7**, pp. 5059-5062, (2004).

[7] J.-P. Ebert and A. Willig, “A Gilbert-Elliott bit-error model and the efficient use in packet level simulation”, Technical report TKN-99-2002, Tech. Univ. Berlin, (1999).

[8] R. Fantacci and M. Scardi, “Performance evaluation of preemptive polling schemes and ARQ techniques for indoor wireless networks”, *IEEE Trans. on Vehicular Tech.*, **vol. 45, no. 2**, pp. 248-257, (1996).

[9] D. Haccoun and G. Begin, “High-rate Punctured Convolutional Codes for Viterbi and Sequential Decoding”, *IEEE Trans. On Comms.*, **vol. 37, no. 11**, pp. 1113-1125, (1989).

[10] I. Haratcherev et al., “Automatic IEEE 802.11 Rate Control for Streaming Applications”, *Wireless Comms. and Mobile Computing*, **vol. 5**, pp. 421-437, (2005).

[11] G. Holland, N. Vaidya, and P. Bahl, “A Rate-Adaptive MAC Protocol for Multi-Hop Wireless Networks”, *ACM/IEEE Mobile Computing and Networking*, pp. 236-251, (2001).

[12] IEEE 802.11 WG, part 11a, *Wireless LAN Medium Access Control (MAC) and Physical Layer (PHY) Specifications*, High-speed Physical Layer in the 5 GHz Band, Standard Specification, IEEE, (1999).

[13] A. Kamerman, L. Monteban, “WaveLAN-II: A High Performance Wireless LAN for the Unlicensed Band”, *Bell Labs. Technical Journal*, Summer, pp. 118-133, (1997).

[14] J. Li and M. Kavehrad, “Effects of Time Selective Multipath Fading on OFDM Systems for Broadband Mobile Applications”, *IEEE Comms. Letters*, **vol. 3, no. 2**, pp. 332-334, (1999).

[15] J. Pavon, S. Choi, “Link Adaptation Strategy for IEEE 802.11 WLAN via Received Signal Strength Measurement”, *IEEE Int. Conf. on Comms.*, **vol. 2**, pp. 1108-1113, (2003).

[16] J. G. Proakis, *Digital Communications*, 4th edition, New York: McGraw-Hill, (2001).

[17] D. Qiao and S. Choi, “Goodput Enhancement of IEEE 802.11a Wireless LAN via Link Adaptation”, *IEEE Int. Conf. on Comms.*, pp. 1995-2000, (2001).

[18] R. Razavi, M. Fleury, and S. Monaghan, “Multimedia Performance for IEEE 802.11 DCF RTS/CTS with Varying Traffic Conditions”, *European Wireless Conf.*, (2007).

[19] R. Steinmetz, “Human Perception of Jitter and Media Synchronization”, *IEEE J. on Selected Areas in Comms.*, **vol. 14, no. 1**, pp. 61-72, (1996).

[20] J. Thomson et al., “An Integrated 802.11a Baseband and MAC Processor”, *IEEE Int. Solid-State Circuits Conference*, **vol. 1**, pp. 126-451, 2002.

[21] H. L. Vu and T. Sakurai, “Accurate delay distribution for IEEE 802.11 DCF”, *IEEE Comms. Letters*, **vol. 10, no. 4**, pp. 317-319, Apr. 2006.

[22] S. Wenger, “H.264/AVC over IP”, *IEEE Trans. on Circuits and Systems for Video Technology*, **vol. 13, no. 7**, pp. 645-655, (2003).

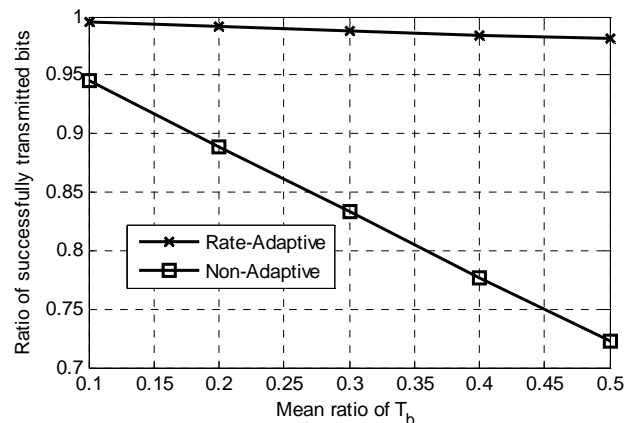


Figure 9: Goodput vs. throughput in a lightly loaded channel (200 packet/s per station).